1018 *Bull. Chem. Soc. Jpn.*, ***78***, *1018–1025 (2005)*

Photochemical Reaction Mechanism of 2,2′-Pyridil in Alcoholic Media

Naoki Yamada, Miki Hasegawa, Ken-ichi Kumagai,* Shigendo Enomoto, Hiroaki Horiuchi,[1]
Tetsutaro Yoshinaga,[2] Hiroshi Hiratsuka,[1] Michio Kobayashi,* and Toshihiko Hoshi

Department of Chemistry and Biological Science, College of Science and Engineering,
Aoyama Gakuin University, Sagamihara, Kanagawa 229-8558

[1]Department of Chemistry, Faculty of Engineering, Gunma University, Kiryu, Gunma 376-8515

[2]Department of Applied Chemistry, Faculty of Engineering, Kyushu Institute of Technology,
Tobata, Kitakyushu, Fukuoka 804-8550

Received December 20, 2004; E-mail: michio@chem.aoyama.ac.jp, ken-ichi@chem.aoyama.ac.jp

Time-resolved transient absorption spectra of photo-irradiated 2,2′-pyridil were measured in PVA films. The broad bands at 552 and ~455 nm, appearing just after photo-excitation of 2,2′-pyridil, are assigned to the skewed triplet species. The triplet species changes into 1-hydroxy-2-oxo-1,2-di(2-pyridyl)ethyl (pyridoil) radical via the abstraction of a hydrogen atom from the solvent. The radical produced by the photo-irradiation of 2,2′-pyridil is confirmed to be the pyridoil radical from the measurement of the polarized absorption spectrum, with the aid of the stretched polymer film technique and MO calculations. The time-resolved transient absorption spectra of 2,2′-pyridil irradiated by a xenon flash lamp in a 1:1 (v/v) mixed solvent of methanol and ethanol show that the pyridoil radical further abstracts a hydrogen atom from the solvent to afford *cis*-enediol (*cis*-1,2-di(2-pyridyl)-1,2-ethenediol) and that *cis*-enediol is converted into *trans*-enediol (*trans*-1,2-di(2-pyridyl)-1,2-ethenediol). 2,2′-Pyridil shows a structured $T_n \leftarrow T_1$ absorption spectrum in a 1:1 (v/v) mixed solvent of methylcyclohexane and 2-methylbutane, indicating that 2,2′-pyridil takes a planar structure in the lowest triplet excited state in a nonpolar medium.

Aromatic α-diketones show very interesting photo-physical and photochemical properties.[1–12] For instance, photo-absorption and emission spectra of α-diketones, which can not be accounted for by the normal Jablonski scheme, indicate that these molecules take skewed structures in the ground states and planar ones in the excited states.[13] Benzil, which is one of the typical α-diketones, is photoreduced to α,α'-dihydroxystilbene in polyhydric alcohols such as ethylene glycol, or glycerol.[11] On the other hand, benzil gives benzoin or other decomposition products such as benzaldehyde by UV light irradiation in the solvents of cyclohexane, 2-propanol, tetrahydrofuran, etc.[2,5,9,10,14] 2,2′-Pyridil (or α-pyridil) shows strong electronic absorption bands in the wavelength region 300–200 nm attributable to allowed $\pi\pi^*$ transitions, and a very weak band in the region 450–320 nm attributable to a forbidden $n\pi^*$ transition.[15–23] Temperature- and solvent-dependent luminescence spectra of 2,2′-pyridil show that this molecule exhibits dual fluorescence and dual phosphorescence that can be ascribed to photorotamerism.[24] According to Inoue et al., 2,2′-pyridil is photoreduced to *trans*-enediol (*trans*-1,2-di(2-pyridyl)-1,2-ethenediol) in alcoholic media, and to *cis*-enediol (*cis*-1,2-di(2-pyridyl)-1,2-ethenediol) in ethereal media.[25,26] It has been found that *trans*-enediol is produced via the lowest triplet excited state of 2,2′-pyridil and *cis*-enediol via the lowest singlet excited one.

The present investigation aims to elucidate the electronic and molecular structure of the reaction intermediate of radical species and the final product enediol, which is produced by the photo-irradiation of 2,2′-pyridil in the stretched PVA film, by measuring the polarized electronic absorption spectra of the two species together with MO calculations. Furthermore, a mechanism for yielding *trans*-enediol will be proposed.

Experimental and MO Calculations

Materials. Commercially available 2,2′-pyridil (Aldrich) was recrystallized five times from ethanol. Methanol (Wako, S grade) was purified by distillation, and ethanol (Wako, S grade) was used as received. 2-Methylbutane was distilled after refluxing with sodium metal. Methylcyclohexane (Dojin, Sp grade) was used without further purification. A 1:1 (v/v) mixed solvent (MP) of methylcyclohexane and 2-methylbutane or a 1:1 (v/v) mixed solvent (ME) of methanol and ethanol was used as a transparent matrix at low temperature. PVA films were prepared by the method already described.[27] In the figures of polarization spectra, Rs is a ratio of stretching of the film and $\mathrm{Rd} = D_{\parallel}/D_{\perp}$. Here, $D_{\parallel}$ and $D_{\perp}$ are optical densities measured with light beams polarized parallel to and perpendicular to the stretching direction, respectively.

Measurements. Electronic absorption spectra were recorded on a Shimadzu UV-3101PC spectrophotometer equipped with a cryostat (Daikin Industries, Model U102W). A Rochon-type polarizer was used for the measurements of polarization spectra. Time-resolved transient absorption spectra were measured with the already described apparatus, in which the photodetecting system with a photomultiplier (Narumi, RM-23) was replaced by a multichannel spectrophotometer with photodiode array (Otsuka Denshi, MCPD-110A).[28]

MO Calculations. In the calculations of transition energies, oscillator strengths and polarization directions, an extended PPP method was employed, being applicable to non-planar molecules

Published on the web June 6, 2005; DOI 10.1246/bcsj.78.1018

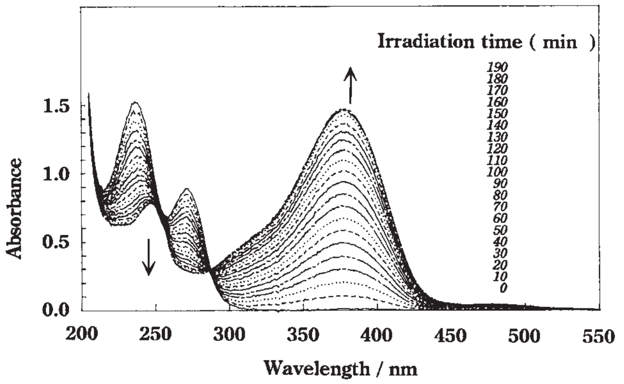

Fig. 1. Changes in $S_n \leftarrow S_0$ absorption spectra caused by a steady light irradiation of 2,2′-pyridil in deoxygenated ethanol at room temperature. The concentration of the solute = 1.15×10^{-4} M.

with nonbonding electron pairs.[29–31] A semiempirical restricted open-shell LCAO-ASMO-SCF-CI method developed by Zahrdnik et al.[32] was used for the open-shell system.[33] A commercially available ab initio program Gaussian 98W (HF/6-31G(d)) (Gaussian Inc.) was used for the calculations of stereo-structures of *cis*- and *trans*-endiols.[34]

Results and Discussion

Transient Absorption Spectra of 2,2′-Pyridil. Figure 1 shows changes in absorption spectra caused by a steady light irradiation of 2,2′-pyridil in deoxygenated ethanol. When 2,2′-pyridil was irradiated by the 270 nm light, the 270.6 and 236.5 nm bands disappeared and new band peaks appeared at 377 and 246.8 nm, along with an additional weak band at around 520–450 nm with an isosbestic point at 286.7 nm. Inoue et al. assigned the electronic bands at 377 and 246.8 nm to *trans*-enediol, but they did not refer to the very weak broad band that appeared in the wavelength region longer than 450 nm.[16,17] This weak band is assigned to the 1-hydroxy-2-oxo-1,2-di(2-pyridyl)ethyl (pyridoil) radical based on a reason described later. Similar spectral changes are observed on the steady light irradiation of 2,2′-pyridil in the PVA film, except that the 270 and 240 nm bands which correspond to the 270.6 and 236.5 nm bands of the mother compound remain but are weak. Figure 2 shows the polarized absorption spectrum of *trans*-enediol (C_{2h} symmetry) in the stretched PVA film measured at 10 K. The 377 and 246.8 nm bands measured in ethanol are shifted to 380 and 248.8 nm in the PVA film, respectively. It is obvious that the 380 nm band with the highest Rd values is polarized longitudinally.[35] Since the Rd curve shows a peak at around 250 nm and two shoulders at ~255 and ~225 nm, these bands are considered to be polarized intermediately or longitudinally. The latter possibility of polarization arises from an overlap of the shorter-axis-polarized intense band of the remaining mother compound. The polarization of the ~310 (320–300) nm shoulder band is transversal or intermediate, because a shoulder in the Rd curve is recognized in this wavelength region. The above-mentioned observations for the electronic bands of *trans*-enediol are compared with the PPP calculated results in Table 1. The calculated transition energies reproduce well the observed band positions, and the calculated oscillator strengths explain qualitatively the relative band intensities, i.e., the observed 380, ~310, ~255, 248.8, and ~225 nm bands are assigned to the calculated transitions to S_1, S_3, S_8, S_{10}, and S_{13} transitions from S_0, respectively. Assuming that the longer molecular axis is along the direction connecting two centers of the pyridine rings, the longitudinal and transversal polarization directions are computed to be 50° and −40° against the central C=C bond axis, respectively (cf. the structure given in Table 1). If this is the case, calculated polarization angles show that all the observed bands are polarized approximately along the longitudinal direction, except that the ~310 nm shoulder band is intermediately polarized.

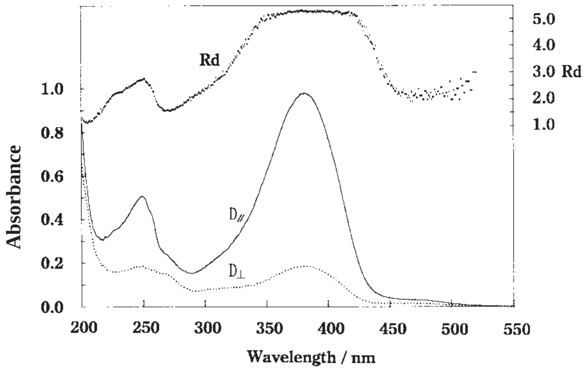

Fig. 2. The polarized $S_n \leftarrow S_0$ absorption spectrum of *trans*-enediol produced by a steady light irradiation of 2,2′-pyridil in the stretched PVA film at 10 K. Rs = 8.88.

While the fluorescence quantum yield of 2,2′-pyridil is small, the phosphorescence quantum yield is very large, indicating that the intersystem crossing occurs effectively.[19,36,37] The lowest singlet excited state of 2,2′-pyridil is assigned to $^1(n\pi^*)$, but no complete assignment is given concerning the lowest triplet excited state.[16–18,21,22,24,36,37] Figure 3 shows time-resolved transient absorption spectra of 2,2′-pyridil measured in the PVA film at 100 K by the xenon flash photolysis method. The spectrum observed at a delay time of 12 ms after the flash light irradiation shows two broad bands peaking at 552 and ~455 nm. Both bands disappear within 50 ms, and new weak bands appear at ~580 and ~480 nm, these weak bands being clearly seen in the spectrum of the inset which is measured at room temperature with the delay time of 12 ms. It is known that photo-irradiation of 2,2′-pyridil gives *trans*-enediol via a triplet state in alcoholic media.[25] Thus, the broad bands at 552 and ~455 nm may be assigned as $T_n \leftarrow T_1$ transitions of 2,2′-pyridil. The weak band at ~480 nm corresponds to the longest weak broad band in Fig. 1 (the band corresponding to the ~580 nm band was too weak to be observed), and is assigned to the pyridoil radical from the following reasons. It is known that α-diketones such as benzil and 2,2′-furil abstract hydrogen from the alcoholic solvent to form ketyl radicals upon photo-irradiation.[38,39] This suggests that a pyridoil radical can be formed from 2,2′-pyridil in the alcoholic solvent upon photo-irradiation, i.e., the ~580 and 488 nm bands observed in the PVA film (Fig. 3 inset) are assigned to the pyridoil radical. Figure 4 shows the polarized transient absorption spectrum of pyridoil radical observed at a delay time of 12 ms in the stretched PVA film at room tem-

Table 1. Comparison of the Calculated and Observed Results for $S_n \leftarrow S_0$ Transitions of *trans*-Enediol

Excited electronic state	Sym.[a]	Transition energy/nm		Intensity		Polarization direction/degree	
		Calcd[b]	Obsd	Calcd[c]	Obsd[d]	Calcd[e]	Obsd[f]
$S_1(\pi^* \leftarrow \pi)$	^1B_u	402.7	380[g](377)[h]	0.805	very strong	36	L
$S_2(\pi^* \leftarrow \pi)$	^1A_g	329.3		forb.[i]		forb.	
$S_3(\pi^* \leftarrow \pi)$	^1B_u	323.1	~310(~310)	0.113	weak	−9	I or S
$S_4(\pi^* \leftarrow \pi)$	^1A_g	292.0		forb.		forb.	
$S_5(\pi^* \leftarrow n)$		290.8		forb.		forb.	
$S_6(\pi^* \leftarrow n)$		290.8		forb.		forb.	
$S_7(\pi^* \leftarrow \pi)$	^1A_g	256.7		forb.		forb.	
$S_8(\pi^* \leftarrow \pi)$	^1B_u	256.2	~255(~255)	0.022	very weak	33	L or I
$S_9(\pi^* \leftarrow \pi)$	^1A_g	228.4		forb.		forb.	
$S_{10}(\pi^* \leftarrow \pi)$	^1B_u	228.4	248.8(246.8)	0.168	strong	38	L or I
$S_{11}(\pi^* \leftarrow n)$		226.7		forb.		forb.	
$S_{12}(\pi^* \leftarrow n)$		226.7		forb.		forb.	
$S_{13}(\pi^* \leftarrow \pi)$	^1B_u	216.2	~225(~225)	0.01	very weak	44	L or I

a) Symmetry: This molecule belongs to a C_{2h} point group and contains the one photon allowed excited states having B_u symmetry with transition moments lying in the molecular XY-plane. b) Excited wavelength (nm) computed with extended PPP method. c) Oscillator strength. d) Relative intensity observed in the stretched PVA film. e) The angle between the central C=C and the transition moment in degree. f) Observed in the stretched PVA film at 10 K (L: longitudinal direction; I: intermediate direction; S: transversal direction.). g) Observed in the stretched PVA film at 10 K. h) Observed in deoxygenated ethanol at room temperature. i) Forbidden transition.

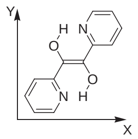

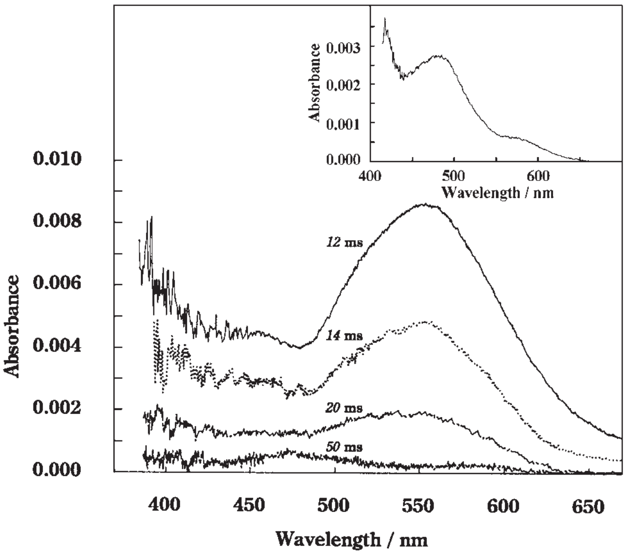

Fig. 3. Time-resolved transient absorption spectra of 2,2′-pyridil in the PVA film at 100 K. Inset: Transient absorption spectrum of 2,2′-pyridil in the PVA film at room temperature measured at delay time 12 ms after flash light irradiation.

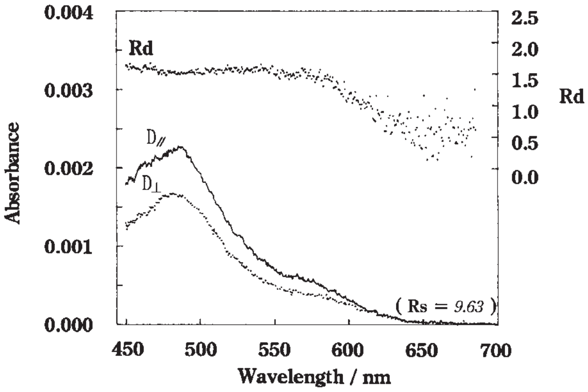

Fig. 4. The polarized transient absorption spectrum of pyridoil radical in the stretched PVA film at room temperature measured at delay time 12 ms after the flash light irradiation.

perature. This spectrum consists of a strong band at 488 nm and a weak shoulder band at ~580 nm. Since the ~580 and 488 nm bands take high Rd values, both bands are considered to be polarized along the longer molecular axis. The Rd curve is lowered on the longer wavelength side of the ~580 nm

Table 2. Comparison of the Calculated and Observed Results for $D_n \leftarrow D_0$ Transitions of Pyridoil Radical

Excited electronic state	Transition energy/nm		Intensity		Polarization direction	
	Calcd[a)]	Obsd[b)]	Calcd[c)]	Obsd[d)]	Calcd[e)]	Obsd[f)]
$D_1(\pi^* \leftarrow \pi)$	457.5	~620	0.001	very weak	S	S
$D_2(\pi^* \leftarrow \pi)$	396.9	~580	0.001	medium	L	L
$D_3(\pi^* \leftarrow \pi)$	357.4		0.000		S	
$D_4(\pi^* \leftarrow \pi)$	342.5	488	0.002	strong	L	L

a) Excited wavelength (nm) computed with semiempirical restricted open-shell LCAO-ASMO-SCF-CI method. b) Observed in the stretched PVA film at room temperature. c) Oscillator strength. d) Relative intensity observed in the stretched PVA film at room temperature. e) L: longitudinal direction; S: transversal direction. f) Observed in the stretched PVA film at 10 K.

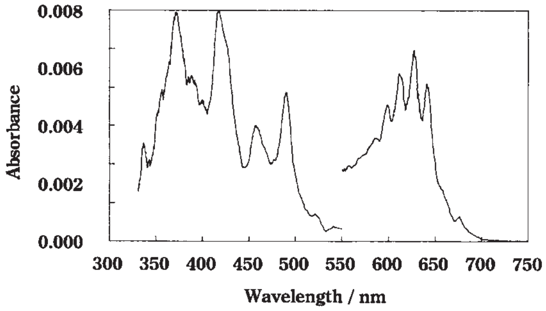

Fig. 5. Transient absorption spectrum of 2,2′-pyridil in MP at 100 K measured at delay time of 12 ms after the flash light irradiation. The concentration of the solute = 1.08×10^{-4} M. The offset at 550 nm is due to a grating change.

Table 3. Comparison of the Calculated and Observed Results for $T_n \leftarrow T_1$ Transitions of the Skewed 2,2′-Pyridil

Excited electronic state	Sym.[a)]	Transition energy/nm		Intensity	
		Calcd[b)]	Obsd[c)]	Calcd[d)]	Obsd[e)]
$T_{23}(\pi^* \leftarrow \pi)$	^3A	442.2	552	0.452	0.009
$T_{24}(\pi^* \leftarrow \pi)$	^3B	442.2		0.137	
$T_{25}(\pi^* \leftarrow \pi)$	^3B	387.8		0.001	
$T_{26}(\pi^* \leftarrow \pi)$	^3A	378.8		0.000	
$T_{27}(\pi^* \leftarrow n_N)$		385.7		forb.[f)]	
$T_{28}(\pi^* \leftarrow n_N)$		385.6		forb.	
$T_{29}(\pi^* \leftarrow \pi)$	^3B	346.6	~455	0.021	0.004
$T_{30}(\pi^* \leftarrow \pi)$	^3A	346.6		0.057	
$T_{31}(\pi^* \leftarrow n_O)$		317.2		0.000	
$T_{32}(\pi^* \leftarrow n_O)$		317.2		0.000	

a) Symmetry: This molecule belongs to a C_2 point group and contains the one photon allowed excited states having A or B symmetry. b) Excited wavelength (nm) computed with extended PPP method. In this calculation, the dihedral angle between two halves of the molecule is 83°. c) Observed in the PVA film at delay time 12 ms after flash irradiation at 100 K. d) Oscillator strength. e) Absorbance observed in the PVA film at delay time 12 ms after flash irradiation at 100 K. f) Forbidden transition.

Table 4. Comparison of the Calculated and Observed Results for $T_n \leftarrow T_1$ Transitions of the s-trans Planar 2,2′-Pyridil

Excited electronic state	Sym.[a)]	Transition energy/nm		Intensity	
		Calcd[b)]	Obsd[c)]	Calcd[d)]	Obsd[e)]
$T_{12}(\pi^* \leftarrow \pi)$	^3B_u	643.6	675	0.022	0.12
$T_{13}(\pi^* \leftarrow \pi)$	^3A_g	640.7		forb.[f)]	
$T_{14}(\pi^* \leftarrow \pi)$	^3B_u	573.3	642	0.203	0.78
$T_{15}(\pi^* \leftarrow n_N)$		470.6		forb.	
$T_{16}(\pi^* \leftarrow n_N)$		470.6		forb.	
$T_{17}(\pi^* \leftarrow \pi)$	^3A_g	464.7		forb.	
$T_{18}(\pi^* \leftarrow \pi)$	^3B_u	413.4	490	0.042	0.74
$T_{19}(\pi^* \leftarrow \pi)$	^3B_u	393.9	457	0.042	0.58
$T_{20}(\pi^* \leftarrow n_N)$		389.6		forb.	
$T_{21}(\pi^* \leftarrow n_N)$		389.6		forb.	
$T_{22}(\pi^* \leftarrow \pi)$	^3A_g	383.0		forb.	
$T_{23}(\pi^* \leftarrow n_O)$		381.7		forb.	
$T_{24}(\pi^* \leftarrow n_O)$		381.7		forb.	
$T_{25}(\pi^* \leftarrow \pi)$	^3A_g	342.7		forb.	
$T_{26}(\pi^* \leftarrow \pi)$	^3B_u	311.0	417	0.279	1.00
$T_{27}(\pi^* \leftarrow \pi)$	^3A_g	291.8		forb.	
$T_{28}(\pi^* \leftarrow n_O)$		289.6		forb.	
$T_{29}(\pi^* \leftarrow n_O)$		289.6		forb.	
$T_{30}(\pi^* \leftarrow n_O)$		287.9		forb.	
$T_{31}(\pi^* \leftarrow n_O)$		287.9		forb.	
$T_{32}(\pi^* \leftarrow n_N)$		280.5		forb.	
$T_{33}(\pi^* \leftarrow n_N)$		280.5		forb.	
$T_{34}(\pi^* \leftarrow \pi)$	^3B_u	280.3	390	0.007	0.82
$T_{35}(\pi^* \leftarrow \pi)$	^3A_g	279.2		forb.	
$T_{36}(\pi^* \leftarrow \pi)$	^3B_u	271.6	371	0.427	1.00

a) Symmetry: This molecule belongs to a C_{2h} point group and contains the one photon allowed excited states having B_u symmetry. b) Excited wavelength (nm) computed with extended PPP method. In this calculation, the dihedral angle between two halves of the molecule is 180°. c) Observed in MP at delay time 12 ms after flash irradiation at 100 K. d) Oscillator strength. e) Relative intensity observed in MP at delay time 12 ms after flash irradiation at 100 K. f) Forbidden transition.

band, indicating that a shorter axis polarized weak band is hidden at around 620 nm. These observations on the pyridoil radical are compared with MO-calculated results in Table 2. The calculated relative transition energies, oscillator strengths and polarization directions explain well the observed ones, i.e., the observed ~620, ~580, and 488 nm bands are assigned to the $D_1 \leftarrow D_0$, $D_2 \leftarrow D_0$, and $D_4 \leftarrow D_0$ transitions, respectively.

As described above, photo-irradiation of 2,2′-pyridil in alcoholic media gives *trans*-enediol.[25] It is interesting to determine the photochemical behavior of 2,2′-pyridil in nonpolar media such as MP for comparison with that in alcoholic media. Figure 5 shows the transient absorption spectrum of 2,2′-pyridil in MP at 100 K measured at the delay time of 12 ms after the flash light irradiation. Each transient band disappears within 500 ms, and the $S_n \leftarrow S_0$ spectrum of the irradiated solution coincides with that of the original solution, indicating that 2,2′-pyridil undergoes no photochemical reaction in MP. Thus, the transient absorption spectrum shown in Fig. 5 is regarded as being due to the $T_n \leftarrow T_1$ transitions of 2,2′-pyridil. It is important to note that the $T_n \leftarrow T_1$ bands observed in MP are accompanied by vibrational fine structures, contrary to the structureless broad ones in alcoholic media (Fig. 3). This indicates that 2,2′-pyridil takes a planar structure in a nonpolar medium MP in the lowest triplet excited state; in contrast, this molecule takes a skewed structure in alcoholic media. The difference in the structures of the lowest triplet excited states in polar and nonpolar media is supported from a difference in lifetimes (τ), i.e., τ (in a nonpolar medium) $= \sim$200 ms and τ (in a polar medium) $= \sim$15 ms. It is known from phosphorescence spectra that α-diketones such as benzil take s-trans planar structures in the lowest triplet excited states in MP.[13] Thus, the $T_n \leftarrow T_1$ spectra in Figs. 3 and 5 are regarded as being due to a skewed and an s-trans planar 2,2′-pyridil, respectively.

To know in more detail the nature of the skewed and s-trans planar triplet species, we have performed extended PPP calculations. The results are compared with observed values in Tables 3 and 4. In the calculations the dihedral angles between two halves of skewed and s-trans planar molecules are assumed to be 83° and 180°, respectively.[19,23,35,40–45] In both cases, the lowest triplet excited states are of $\pi\pi^*$ character, different from the case of benzil.[46] Relatively intense electronic transitions are computed at 442.2 and 346.6 nm for the skewed triplet species, and at 573.3, 413.4, 393.9, 311.0, and 271.6 nm for the s-trans planar one. The former results explain well the spectrum in Fig. 3, and the latter results explain the spectrum in Fig. 5. The 552 nm band of the skewed triplet species is assigned to the overlap of the $T_{23} \leftarrow T_1$ and $T_{24} \leftarrow T_1$ transitions, and the ~455 nm band to that of the $T_{29} \leftarrow T_1$ and $T_{30} \leftarrow T_1$ transitions (Table 3). The 675, 642, 490, 457, 417, 390, and 371 nm bands of the s-trans planar triplet species are assigned to the transitions to T_{12}, T_{14}, T_{18}, T_{19}, T_{26}, T_{34}, and T_{36} from T_1, respectively (Table 4).

The Mechanism of the *trans*-Enediol Formation in Alcoholic Media. In order to determine the reaction mechanism of *trans*-enediol produced by the steady light irradiation of 2,2′-pyridil in alcoholic media (Fig. 1), we have measured time-resolved transient absorption spectra of 2,2′-pyridil in ME at room temperature (Fig. 6). The band assigned to pyridoil radical in the wavelength region 550–430 nm is weakened with a lapse of time, and disappears at the delay time of 5100 ms (cf.

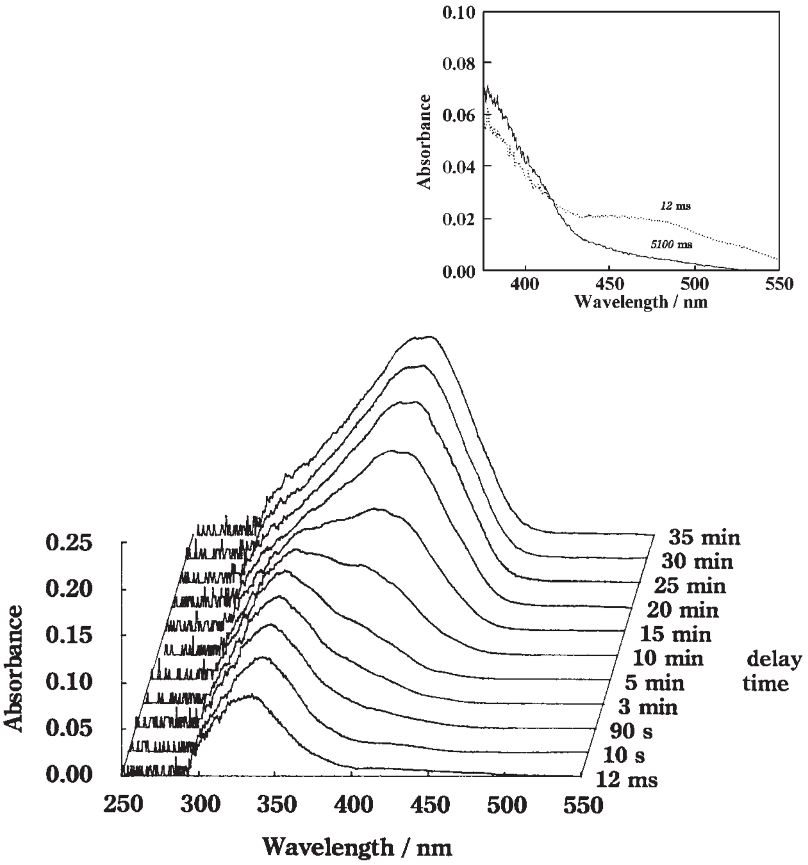

Fig. 6. Time-resolved transient absorption spectra of 2,2′-pyridil in ME at room temperature. The concentration of the solute = 2.70×10^{-3} M. Inset: Time-resolved transient absorption spectra of 2,2′-pyridil in ME at 100 K. The concentration of the solution = 1.00×10^{-3} M.

inset in Fig. 6). The band at ~340 nm is weakened and a new band appears at ~400 nm with a lapse of time, keeping an isosbestic point at 345 nm. Photo-irradiation of 2,2′-pyridil in ethereal media yields *cis*-enediol, exhibiting an absorption peak at ~340 nm.[26] From the band shapes and positions, the ~340 nm band observed at 12 ms is considered to be due to *cis*-enediol, and the newly-appearing ~400 nm band (corresponding to the 380 nm band measured in ethanol) to *trans*-enediol. It is clarified, therefore, that *cis*-enediol is formed primarily by the photo-irradiation even in alcoholic media, and this *cis*-enediol is converted into *trans*-enediol thermally with the passage of time. The initially formed *cis*-enediol is almost completely converted into *trans*-enediol after 35 min. The present extended PPP calculated results also support the above argument. That is, for instance, the first transition energies for *cis*- and *trans*-enediols are computed to be 364 and 403 nm, respectively. In this calculation, a skewed geometry, which is obtained from ab initio calculations as described below, has been employed for *cis*-enediol.

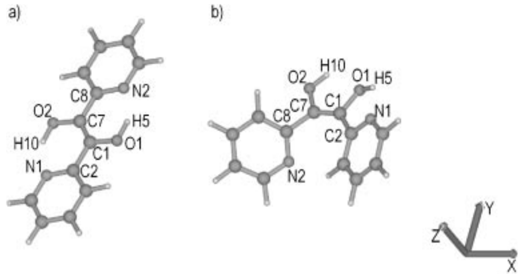

Fig. 7. The optimized structure, obtained by ab initio (HF/6-31G(d)) calculations, of *trans*- (a) and *cis*-enediols (b).

In order to clarify the stereo-structures of *cis*- and *trans*-enediols, we have performed ab initio calculations. In the present geometry-optimized calculations, various kinds of starting structures for both enediols have been assumed: twenty two kinds of planar and non-planar structures for *cis*-enediol, and five planar (except hydroxy hydrogen atoms) structures for *trans*-enediol. The most stable structures for both enediols are shown in Fig. 7: i.e., *trans*-enediol is predicted to take a C_2 structure (almost planar including hydrogen atoms), and *cis*-enediol to take a skewed structure in which one pyridyl plane is twisted by 30° around the C1–C2 bond axis from the planar structure and the other one is twisted by 40° around the C7–C8 bond axis. In the cis form, the H5 hydrogen atom is considered to be H-bonded to the N1 nitrogen atom, and, in the trans form, the H5 and H10 hydrogen atoms are considered to be H-bonded to the N2 and N1 nitrogen atoms, respectively. The present ab initio calculations show that the planar *trans*-enediol is more stable than the skewed *cis*-one by 51 kJ·mol^{-1}.

Concluding Remarks

The above experimental results are summarized in Fig. 8. In alcoholic media a skewed lowest triplet $\pi\pi^*$ excited species is formed via a skewed $^1(n\pi^*)$ state through the intersystem crossing. This triplet species abstracts a hydrogen atom from the solvent to afford a pyridoil radical, and the pyridoil radical abstracts one more hydrogen atom to yield *cis*-enediol. Finally, the *cis*-enediol converts into *trans*-enediol thermally. Scaiano reported that xanthone abstracts effectively hydrogen atoms from alcoholic solvents in the lowest triplet excited $n\pi^*$ state.[47] As described above, the lowest triplet excited state of 2,2′-pyridil is of $\pi\pi^*$, but this molecule abstracts hydrogen

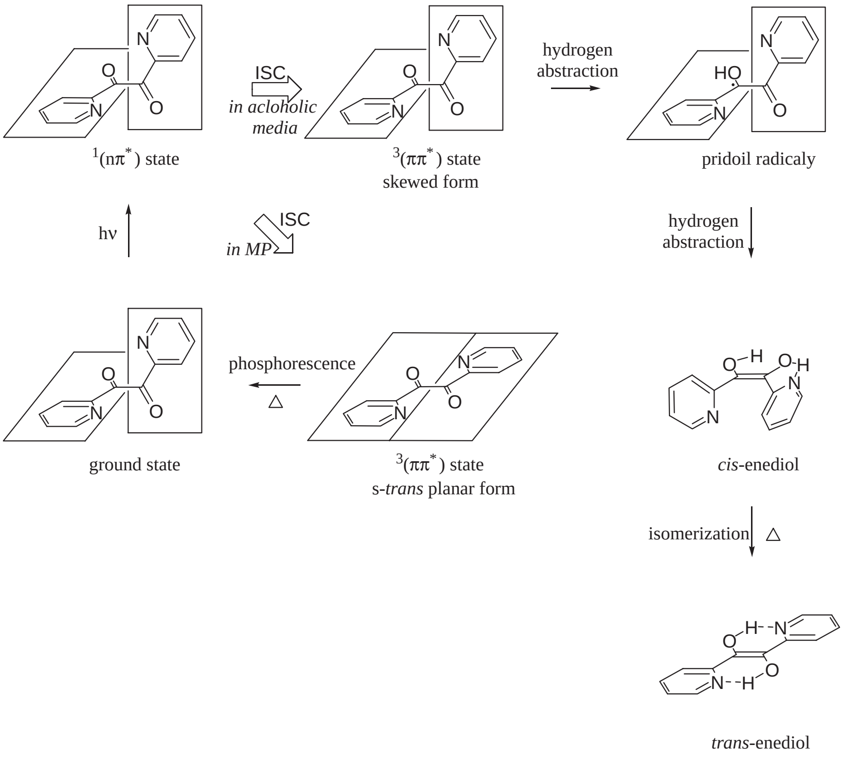

Fig. 8. A proposed primary photochemical reaction process of 2,2′-pyridil.

atoms from alcoholic solvents, as seen in Fig. 8. This may be interpreted to mean that the lowest $^3(\pi\pi^*)$ excited state of 2,2′-pyridil partially gains an nπ^* character due to a mixing of $^3(\pi\pi^*)$ and $^3(\mathrm{n}\pi^*)$ configurations of 2,2′-pyridil, because this molecule takes a skewed structure in the lowest $^3(\pi\pi^*)$ excited state in alcoholic solvents, with the n and π orbitals being not orthogonal. On the other hand, since 2,2′-pyridil takes a planar structure in the lowest $^3(\pi\pi^*)$ excited state in non-polar media, the mixing between $^3(\pi\pi^*)$ and $^3(\mathrm{n}\pi^*)$ configurations does not occur due to orthogonality of n and π orbitals, making hydrogen abstraction impossible. The skewed triplet species shows electronic absorption bands at 552 and ~455 nm in the PVA film at 100 K, and the pyridoil radical at 620, 580, and 488 nm in the PVA film at room temperature. *cis*-Enediol shows electronic bands at ~340 nm, and *trans*-enediol shows them at ~400 nm in ME at room temperature. In nonpolar solvent MP, photo-irradiation of 2,2′-pyridil gives an s-trans planar triplet $\pi\pi^*$ excited species with electronic absorption peaks at 675, 642, 490, 457, 417, 390, and 371 nm; this triplet species returns to the ground state without any photochemical reaction.

References

1 M. B. Rubin and R. G. LaBarge, *J. Org. Chem.*, **31**, 3283 (1966).

2 D. L. Bunbury and C. T. Wang, *Can. J. Chem.*, **46**, 1473 (1968).

3 P. A. Carapellucci, H. P. Wolf, and K. Weiss, *J. Am. Chem. Soc.*, **91**, 4635 (1969).

4 B. M. Monroe and S. A. Weiner, *J. Am. Chem. Soc.*, **91**, 450 (1969).

5 D. L. Bunbury and T. T. Chung, *Can. J. Chem.*, **47**, 2045 (1969).

6 R. G. Zepp and P. J. Wagner, *J. Am. Chem. Soc.*, **92**, 7466 (1970).

7 N. J. Turro and T.-J. Lee, *J. Am. Chem. Soc.*, **92**, 7467 (1970).

8 H. Inoue, T. Nakamura, and T. Igarashi, *Bull. Chem. Soc. Jpn.*, **44**, 1469 (1971).

9 D. L. Bunbury and T. M. Chan, *Can. J. Chem.*, **50**, 2499 (1972).

10 K. Maruyama, K. Ono, and J. Osugi, *Bull. Chem. Soc. Jpn.*, **45**, 847 (1972).

11 H. Inoue, S. Takido, T. Somemiya, and Y. Nomura, *Tetrahedron Lett.*, **1973**, 2755.

12 P. J. Wagner, R. G. Zepp, K.-C. Liu, M. Thomas, T.-J. Lee, and N. J. Turro, *J. Am. Chem. Soc.*, **98**, 8125 (1976).

13 D. J. Morantz and A. J. C. Wright, *J. Chem. Phys.*, **54**, 692 (1971).

14 T. Caceres, M. V. Encinas, and E. A. Lissi, *J. Photochem.*, **27**, 109 (1984).

15 N. J. Leonard and E. R. Blout, *J. Am. Chem. Soc.*, **72**, 484 (1950).

16 W. Mathes, W. Sauermilch, and Th. Klein, *Chem. Ber.*, **84**, 452 (1951).

17 B. Eistert and H. Munder, *Chem. Ber.*, **88**, 215 (1955).

18 F. Bottari and C. Salvatore, *Gazz. Chim. Ital.*, **87**, 1281 (1957).

19 I. Bernal, *Nature*, **200**, 1318 (1963).

20 A. Heller and E. Wasserman, *J. Chem. Phys.*, **42**, 949 (1965).

21 S. C. Bera, R. K. Mukherjee, D. Mukherjee, and M. Chowdhury, *J. Chem. Phys.*, **55**, 5826 (1971).

22 H. Inoue and K. Nagaya, *J. Chem. Soc., Perkin Trans. 2*, **1983**, 1581.

23 T. Hoshi, J. Okubo, I. Ono, S. Watanabe, H. Inoue, T. Sakurai, and M. Kobayashi, *Nippon Kagaku Kaishi*, **1990**, 655.

24 A. Sarkar and S. Chakravorti, *J. Lumin.*, **69**, 161 (1996).

25 H. Inoue, T. Sakurai, T. Hoshi, I. Ono, and J. Okubo, *J. Photochem. Photobiol., A*, **60**, 121 (1991).

26 H. Inoue, T. Sakurai, T. Hoshi, and J. Okubo, *J. Photochem. Photobiol., A*, **72**, 41 (1993).

27 T. Hoshi, H. Yamamoto, T. Miyauchi, S. Mori, M. Kobayashi, and Y. Tanizaki, *Ber. Bunsen-Ges. Phys. Chem.*, **86**, 330 (1982).

28 T. Hoshi, K. Ota, J. Yoshino, K. Murofushi, and Y. Tanizaki, *Chem. Lett.*, **1977**, 357.

29 T. Hoshi, M. Kobayashi, J. Yoshino, M. Komuro, and Y. Tanizaki, *Ber. Bunsen-Ges. Phys. Chem.*, **83**, 821 (1979).

30 T. Hoshi, Y. Inomaki, M. Wada, Y. Yamada, J. Okubo, M. Kobayashi, and H. Inoue, *Ber. Bunsen-Ges. Phys. Chem.*, **98**, 585 (1994).

31 K. Kumagai, M. Hasegawa, J. Okubo, and T. Hoshi, *Nippon Kagaku Kaishi*, **2001**, 507.

32 R. Zahradnik and P. Carsky, *J. Phys. Chem.*, **74**, 1235 (1970).

33 T. Hoshi, J. Okubo, N. Yamamoto, and S. Tanabe, *Ber. Bunsen-Ges. Phys. Chem.*, **91**, 1069 (1987).

34 "Gaussian 98, Revision A.9," M. J. Frisch, G. W. Trucks, H. B. Schlegel, G. E. Scuseria, M. A. Robb, J. R. Cheeseman, V. G. Zakrzewski, J. A. Montgomery, Jr., R. E. Stratmann, J. C. Burant, S. Dapprich, J. M. Millam, A. D. Daniels, K. N. Kudin, M. C. Strain, O. Farkas, J. Tomasi, V. Barone, M. Cossi, R. Cammi, B. Mennucci, C. Pomelli, C. Adamo, S. Clifford, J. Ochterski, G. A. Petersson, P. Y. Ayala, Q. Cui, K. Morokuma, D. K. Malick, A. D. Rabuck, K. Raghavachari, J. B. Foresman, J. Cioslowski, J. V. Ortiz, A. G. Baboul, B. B. Stefanov, G. Liu, A. Liashenko, P. Piskorz, I. Komaromi, R. Gomperts, R. L. Martin, D. J. Fox, T. Keith, M. A. Al-Laham, C. Y. Peng, A. Nanayakkara, M. Challacombe, P. M. W. Gill, B. Johnson, W. Chen, M. W. Wong, J. L. Andres, C. Gonzalez, M. Head-Gordon, E. S. Replogle, and J. A. Pople, Gaussian, Inc., Pittsburgh PA (1998).

35 Y. Tanizaki, H. Inoue, T. Hoshi, and J. Shiraishi, *Z. Phys. Chem. (Neue Folge)*, **74**, 45 (1971).

36 V. L. Ermolaev, *Opt. Spectrosc.*, **1**, 523 (1956).

37 T. R. Evans and P. A. Leermakers, *J. Am. Chem. Soc.*, **89**, 4380 (1967).

38 A. J. Elliot and J. K. S. Wan, *Can. J. Chem.*, **56**, 2499 (1978).

39 G. Krishna, D. Mohapatra, J. Bhattacharya, J. Bandopadhyay, and S. C. Bera, *J. Photochem. Photobiol., A*, **40**, 47 (1987).

40 S. Hirokawa and T. Ashida, *Acta Crystallogr.*, **14**, 774 (1961).

41 J. Barassin, *Ann. Chim. (Paris)*, **8**, 637 (1963).

42 W. G. Herkstroeter, J. Saltiel, and G. S. Hammond, *J. Am. Chem. Soc.*, **85**, 482 (1963).

43 R. J. W. Le Fevre and P. J. Stiles, *J. Chem. Soc. B*, **1966**, 420.

44 T. Ashida and S. Hirokawa, *Acta Crystallogr., Sect. B*, **26**, 454 (1970).

45 P. Migchels, G. Maes, Th. Zeegers-Huyskens, and M. Rospenk, *J. Mol. Struct.*, **193**, 223 (1989).

46 N. Locoge, G. Buntinx, N. Ratovelomanana, and O. Poizat, *J. Phys. Chem.*, **96**, 1106 (1992).

47 J. C. Scaiano, *J. Am. Chem. Soc.*, **102**, 7747 (1980).